

Ferromagnetic interlayer exchange coupling in semiconductor SbCrTe/Sb₂Te₃/SbCrTe trilayer structures

Zhenhua Zhou,^{a)} Yi-Jiunn Chien, and Ctirad Uher

Department of Physics, University of Michigan, Ann Arbor, Michigan 48109

(Received 8 August 2006; accepted 16 October 2006; published online 4 December 2006)

Semiconductor trilayer structures with ferromagnetic Sb_{2-x}Cr_xTe₃ layers separated by a nonmagnetic Sb₂Te₃ layer of different thickness have been fabricated by molecular beam epitaxy. Ferromagnetic out-of-plane exchange coupling between the SbCrTe layers was found and the coupling strength, which can be represented by a saturation field H_S , depends on both the Sb₂Te₃ spacer thickness and temperature. © 2006 American Institute of Physics. [DOI: 10.1063/1.2398905]

Since the discovery of antiferromagnetic interlayer exchange coupling between ferromagnetic metals separated by a nonmagnetic metal or semiconductor spacers,¹⁻⁵ investigations of this kind have been extended to the so-called all-semiconductor trilayer structures which typically represent two ferromagnetic semiconductor layers separated by a semiconductor or insulator layer with a specific thickness. The interlayer exchange coupling (IEC) between the ferromagnetic layers through the nonmagnetic layer has been the focus of investigations. IEC between two ferromagnets separated by a nonmagnetic metal spacer has been studied both theoretically^{6,7} and experimentally.¹⁻³ By replacing metallic ferromagnets with ferromagnetic semiconductors and the metallic spacer with a semiconductor, the so-called all-semiconductor $F/N/F$ trilayer structure can be fabricated and used to investigate the IEC in semiconductor nanostructures. So far, IEC in all-semiconductor $F/N/F$ trilayer structures has only been studied in GaMnAs/AlGaAs/GaMnAs (Refs. 8–11) and InMnAs/InAs/InMnAs (Ref. 12) systems through tunneling magnetoresistance investigations. IEC in magnetic semiconductor nanostructures as a function of temperature and spacer thickness can also be studied with Hall effect measurements since abnormal Hall resistivity of a magnetic thin film is proportional to the magnetization which includes the IEC between the ferromagnetic layers.

Recently, we reported on the preparation and magnetic properties of Sb_{2-x}V_xTe₃ and Sb_{2-x}Cr_xTe₃ in the form of thin films fabricated by the low-temperature molecular beam epitaxy (LT-MBE) growth.^{13,14} The concentration of V and Cr in Sb_{2-x}V_xTe₃ and Sb_{2-x}Cr_xTe₃ was increased to $x=0.35$ and $x=0.59$, respectively. This is an order of magnitude higher concentration of transition metal (TM) ions than that in bulk single crystals of Sb_{2-x}V_xTe₃ (Ref. 15) and Sb_{2-x}Cr_xTe₃,^{16,17} where the solubility of transition metals is very low, typically on the order of $x < 0.05$. In spite of this low concentration of TMs, the bulk tetradymite-type Sb₂Te₃ semiconductors doped with either V or Cr were shown to support ferromagnetism to temperatures of about 25 K. Since the Curie temperature depends strongly on the concentration of TM ions, the enhanced solubility of TMs achieved in thin film forms of Sb₂Te₃ has resulted in a dramatically extended regime of ferromagnetism to temperatures of 177 and 190 K for thin

film samples of Sb_{1.65}Cr_{0.35}Te₃ (Ref. 13) and Sb_{1.41}V_{0.59}Te₃,¹⁴ respectively. These high Curie temperatures encourage us to explore the nature of IEC in semiconductor $F/N/F$ trilayer structures based on Sb₂Te₃ for possible future applications in spintronic devices. In this letter, we report on results concerning the growth and transport properties of $F/N/F$ trilayer nanostructures based on Sb_{2-x}Cr_xTe₃/Sb₂Te₃/Sb_{2-y}Cr_yTe₃ prepared by LT-MBE.

The trilayer structure Sb_{2-x}Cr_xTe₃/Sb₂Te₃/Sb_{2-y}Cr_yTe₃ comprises top and bottom Cr-doped Sb₂Te₃ layers with a pure Sb₂Te₃ layer spacer sandwiched in between. After first growing a layer of Sb_{2-x}Cr_xTe₃ on a sapphire substrate, the Cr flux is blocked in order to deposit the Sb₂Te₃ spacer layer of various thicknesses. By opening the shutter in front of the Cr source again and adjusting the power of the e-beam evaporator, the second Sb_{2-y}Cr_yTe₃ layer with a different Cr concentration is grown on top of the Sb₂Te₃ spacer layer. We fabricated the above trilayer structures with different spacer thicknesses (10, 4, 2, 0 nm), while the thickness of both Cr-doped Sb₂Te₃ layers was kept at about 50 nm. Based on our observation that the Sb₂Te₃ films grow on sapphire sub-

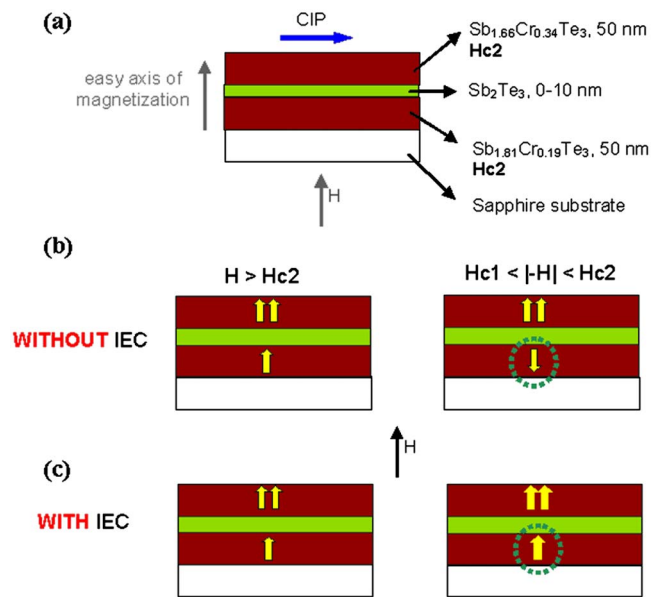


FIG. 1. (Color online) (a) Schematic of the $F/N/F$ trilayer structure based on Sb_{2-x}Cr_xTe₃/Sb₂Te₃/Sb_{2-y}Cr_yTe₃. (b) Schematic of the spin configuration of the $F/N/F$ trilayer without IEC. (c) Schematic of the spin configuration of the $F/N/F$ trilayer with IEC.

^{a)} Author to whom correspondence should be addressed; present address: Delphi Corporation Research Labs, 51786 Shelby Parkway, Shelby Township, MI 48315; electronic mail: zhenhua.zhou@delphi.com

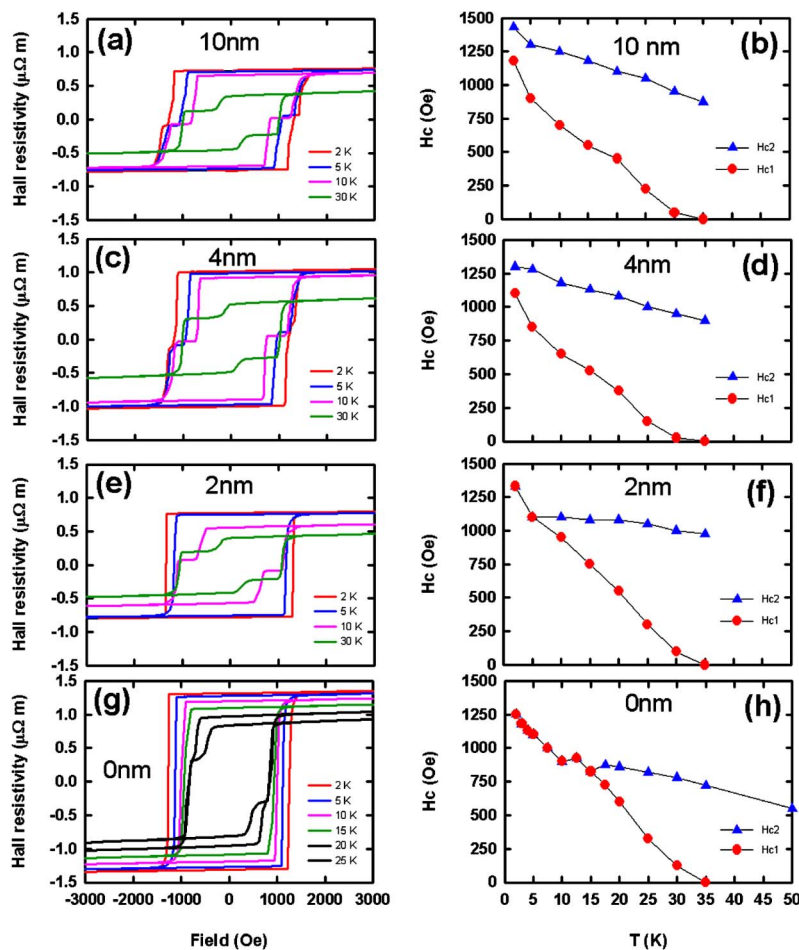


FIG. 2. (Color online) Magnetic field dependent Hall resistivity for $Sb_{1.66}Cr_{0.34}Te_3/Sb_2Te_3/Sb_{1.81}Cr_{0.19}Te_3$ trilayer structures with various spacer thickness: (a) 10 nm, (c) 4 nm, (e) 2 nm, and (g) 0 nm. Coercive fields as a function of temperature for $Sb_{1.66}Cr_{0.34}Te_3/Sb_2Te_3/Sb_{1.81}Cr_{0.19}Te_3$ trilayer structures with various spacer thickness: (b) 10 nm, (d) 4 nm, (f) 2 nm, and (h) 0 nm.

strates in a substantially layer-by-layer fashion¹⁸ and are continuous down to at least 2 nm, we believe that the spacer layer of Sb_2Te_3 is free of pinholes. The concentration of Cr in the top and bottom layers is kept at $x=0.34\pm 0.01$ and $x=0.19\pm 0.01$, respectively.

Figure 1(a) shows a schematic of the $F/N/F$ trilayer nanostructure based on Sb_2Te_3 . Two ferromagnetic layers, $Sb_{1.66}Cr_{0.34}Te_3$ on the top and $Sb_{1.81}Cr_{0.19}Te_3$ at the bottom, are separated by a thin layer of nonmagnetic Sb_2Te_3 the thickness of which is varied from 0 to 10 nm. H_{c1} and H_{c2} are the coercive fields of $Sb_{1.81}Cr_{0.19}Te_3$ and $Sb_{1.66}Cr_{0.34}Te_3$ blocks, respectively, at a given temperature. Measurements of the individual films of $Sb_{1.81}Cr_{0.19}Te_3$ and $Sb_{1.66}Cr_{0.34}Te_3$ show that the Curie temperatures are 67 and 106 K, respectively. When the trilayer structure is cooled below the Curie temperature, its magnetic behavior is determined not only by the Cr-doped Sb_2Te_3 layers but also by the IEC between these layers. As shown in Fig. 1(b), when there is *no* IEC between the top and bottom layers, the total magnetization of the trilayer structure will be simply the sum of these two layers' magnetizations which are not correlated. If initially a high magnetic field (pointing up) is applied to saturate the trilayer structure and then the magnetic field is gradually reduced, the following behavior should be observed: (1) when $|H| > H_{c2}$, and since $H_{c2} > H_{c1}$, the spins in both the top and bottom Cr-doped Sb_2Te_3 layers will be aligned with the direction of the external magnetic field; (2) when the magnetic field is further reduced and reversed until it satisfies $H_{c1} < |-H| < H_{c2}$, the spins in the top $SbCrTe$ layer will still be aligned parallel to the original direction of the magnetic

field, but the spins in the bottom layer will be reversed, i.e., pointing down. Therefore, the total magnetization will be reduced. A *two-step* decrease of the total magnetization will be observed as a result of sequential alignments of the spins in the bottom and top layers by the external magnetic field.

Let us now consider that there is *ferromagnetic* IEC acting between the top and bottom Cr-doped Sb_2Te_3 layers, a situation depicted in Fig. 1(c). In this case, the total magnetization of the trilayer structure will be determined by the sum of the magnetizations of the top and bottom layers plus the contribution from the ferromagnetic IEC. The ferromagnetic IEC correlates the magnetic moments of the top and bottom layers, and now these two magnetizations behave like a single moment instead of two uncorrelated moments such as those in Fig. 1(b). If a high magnetic field is applied to saturate the trilayer structure (assume again the direction of the external field is up) and then the field is gradually reduced, one should observe the following behavior: (1) when $|H| > H_{c2}$, and since $H_{c2} > H_{c1}$, the spins in both the top and bottom Cr-doped Sb_2Te_3 layers will be aligned with the direction of the external magnetic field; (2) when the magnetic field is reduced and reversed and it satisfies $H_{c1} < |-H| < H_{c2}$, the spins in the top layer obviously remain aligned to the original direction of the magnetic field and point up, and the spins in the bottom layer will also point up instead of down due to the ferromagnetic IEC between these two layers. The total magnetization of such a trilayer structure will be larger than that without ferromagnetic IEC. Therefore, the field dependence of magnetization will indicate whether there is ferromagnetic IEC or not in the trilayer structure.

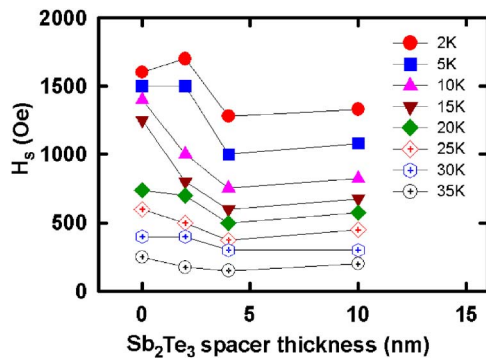


FIG. 3. (Color online) Saturation field H_S as a function of temperature and Sb_2Te_3 spacer thickness.

Temperature dependent Hall resistivity of $\text{Sb}_{1.66}\text{Cr}_{0.34}\text{Te}_3/\text{Sb}_2\text{Te}_3/\text{Sb}_{1.81}\text{Cr}_{0.19}\text{Te}_3$ trilayer structures has been measured using an ac bridge with 16 Hz excitation. Figures 2(a), 2(c), 2(e), and 2(g) show the magnetic field dependent Hall resistivity of the $\text{Sb}_{1.66}\text{Cr}_{0.34}\text{Te}_3/\text{Sb}_2\text{Te}_3/\text{Sb}_{1.81}\text{Cr}_{0.19}\text{Te}_3$ trilayer structures taken at different temperatures and for the Sb_2Te_3 spacer thicknesses of 10, 4, 2, and 0 nm, respectively. For samples with the Sb_2Te_3 spacer layer thickness of 10 nm [Fig. 2(a)] and 4 nm [Fig. 2(c)], the Hall resistivity undergoes a two-step decrease when the magnetic field is reduced from 5 T and reversed, i.e., the spins in the top and bottom layers are rotated by the magnetic field *separately* at all temperatures down to 2 K. There is no ferromagnetic IEC in such trilayers since the top and bottom layers respond to the magnetic field separately. For samples with the Sb_2Te_3 spacer layer thicknesses of 2 nm [Fig. 2(e)] and 0 nm [Fig. 2(g)], there exists a critical temperature which tends to increase with the decreasing Sb_2Te_3 spacer thickness. Below that critical temperature, the Hall resistivity undergoes only *one-step* transition when the magnetic field is reduced from 5 T and reversed, i.e., the spins in the top and bottom layers are rotated by the magnetic field in unison. The critical temperature is about 5 K for a sample with the Sb_2Te_3 spacer thickness of 2 nm and 15 K for a sample with the Sb_2Te_3 spacer thickness of 0 nm. The correlated behavior of the spins in both the top and bottom Cr-doped Sb_2Te_3 layers indicates that there is a strong ferromagnetic interlayer exchange coupling between the layers through the Sb_2Te_3 spacer when the thickness of the latter is small enough.

The strength of IEC between the ferromagnetic layers depends on several parameters that include but are not limited to the magnetization and thickness of the ferromagnetic layers. According to Parkin *et al.*,³ an experimental measure of the strength of *antiferromagnetic* IEC includes the so-called saturation field H_S , which is the field at which the magnetization curve first deviates from the high field slope. This field marks the strength of the antiferromagnetic IEC. The above authors then defined the strength of IEC in Co/Cr, Co/Ru, and Fe/Cr superlattices to be $H_S M t_f$, where H_S , M , and t_f are the saturation field, magnetization, and thickness of the ferromagnetic layer, respectively. For ferromagnetic IEC in $F/N/F$ trilayer structures, such definition is also valid since the saturation field H_S indicates the complete rotation and alignment of the ferromagnetically correlated spins in both F layers. H_S at 2 K is indicated with arrows in

Figs. 2(a), 2(c), 2(e), and 2(g). Since the anomalous Hall resistivity is proportional to the magnetization, the field at which the Hall data depart from the high field slope is the signature of the first deviation of magnetization from the high field slope. For a fixed ferromagnetic layer thickness and temperature, the ICE strength is a function of H_S only. Therefore, H_S can be used as a measure of the interlayer exchange coupling between the Cr-doped Sb_2Te_3 layers through the Sb_2Te_3 layer. Figure 3 plots the dependence of H_S on the Sb_2Te_3 spacer thickness at temperatures ranging from 2 to 35 K. It is clear that the strength of ferromagnetic IEC in $\text{Sb}_{2-x}\text{Cr}_x\text{Te}_3/\text{Sb}_2\text{Te}_3/\text{Sb}_{2-y}\text{Cr}_y\text{Te}_3$ trilayer structures is both temperature and spacer thickness dependent. H_S tends to decrease with increasing temperature, but shows a complicated dependence on the spacer thickness. It is not clear at this moment whether the dependence of H_S on the spacer thickness at low temperature (≤ 25 K) is of oscillatory nature or not. More data points at various spacer thicknesses will be required to address this issue.

In summary, ferromagnetic interlayer exchange coupling was found in semiconductor $\text{Sb}_{1.66}\text{Cr}_{0.34}\text{Te}_3/\text{Sb}_2\text{Te}_3/\text{Sb}_{1.81}\text{Cr}_{0.19}\text{Te}_3$ trilayers as a function of both the Sb_2Te_3 spacer thickness and the temperature. At low temperatures and for small thickness of the spacer layer, the ferromagnetic IEC couples the two ferromagnetic layers and the entire trilayer structure behaves like a single magnetic layer. This finding opens the door for future applications of semiconductor spintronics based on the Sb_2Te_3 system such as ultra-high density perpendicular magnetic recording that is being investigated.

This work was supported by National Science Foundation Grants No. NSF-DMR-0305221 and NSF-DMR-0604549.

- ¹P. Gruenberg, R. Schreiber, Y. Pang, M. B. Brodsky, and H. Sowers, Phys. Rev. Lett. **57**, 2442 (1986).
- ²M. N. Baibich, J. M. Broto, A. Fert, F. Nguyen Van Dau, F. Petroff, P. Eitenne, G. Creuzet, A. Friederich, and J. Chazelas, Phys. Rev. Lett. **61**, 2472 (1988).
- ³S. S. P. Parkin, N. More, and K. P. Roche, Phys. Rev. Lett. **64**, 2304 (1990).
- ⁴R. R. Gareev, D. E. Buegler, M. Buchmeier, D. Olligs, R. Schreiber, and P. Gruenberg, Phys. Rev. Lett. **87**, 157202 (2001).
- ⁵Z. Y. Liu and S. Adenwalla, Phys. Rev. Lett. **91**, 037207 (2003).
- ⁶P. Bruno, Phys. Rev. B **52**, 411 (1995).
- ⁷L. L. Hinchey and D. L. Mills, Phys. Rev. B **33**, 3329 (1986).
- ⁸N. Akiba, F. Matsukura, A. Shen, Y. Ohno, H. Ohno, A. Oiwa, S. Katsunoto, and Y. Iye, Appl. Phys. Lett. **73**, 2122 (1998).
- ⁹D. Chiba, N. Akiba, F. Matsukura, Y. Ohno, and H. Ohno, Appl. Phys. Lett. **77**, 1873 (2000).
- ¹⁰S. J. Chung, S. Lee, I. W. Park, X. Liu, and J. K. Furdyna, J. Appl. Phys. **95**, 7402 (2004).
- ¹¹P. Sankowski and P. Kacman, Phys. Rev. B **71**, 201303(R) (2005).
- ¹²S. Yanagi, H. Muneakata, Y. Kitamoto, A. Oiwa, and T. Slupinski, J. Appl. Phys. **91**, 7902 (2002).
- ¹³Z. Zhou, Y.-J. Chien, and C. Uher, Appl. Phys. Lett. **87**, 112503 (2005).
- ¹⁴Z. Zhou, Y.-J. Chien, and C. Uher, Phys. Rev. B (to be published).
- ¹⁵J. S. Dyck, P. Hájek, P. Lošták, and C. Uher, Phys. Rev. B **65**, 115212 (2002).
- ¹⁶J. S. Dyck, Č. Drašar, P. Lošták, and C. Uher, Phys. Rev. B **71**, 115214 (2005).
- ¹⁷V. A. Kulbachinskii, A. Yu. Kaminskii, K. Kindo, Y. Narumi, K. Suga, P. Lošták, and P. Švanda, JETP Lett. **73**, 352 (2001).
- ¹⁸Y.-J. Chien, Z. Zhou, and C. Uher, J. Cryst. Growth **283**, 309 (2005).